protein expression. In contrast, neither BDNF nor TrkB-Fc was able to modulate myelin protein expression when injected into the $p75^{NTR-/-}$ mice, in agreement with the premise that $p75^{NTR}$ is the functional receptor for BDNF. The lack of BDNF activity was in sharp contrast with that of NT3. In both wild-type and $p75^{NTR-/-}$ mice, injection with NT3 inhibited myelination and injection with TrkC-Fc enhanced myelination to the same degree. Similar conclusions were obtained with mouse SC/DRG cocultures (*12*). Myelin protein expression was enhanced by BDNF and decreased by TrkB-Fc in myelinating cocultures from wild-type embryos (Fig. 3, C and D), whereas neither BDNF nor TrkB-Fc had any effect in cocultures from $p75^{NTR-/-}$ embryos. Furthermore, NT3 inhibited and TrkC-Fc enhanced myelination in both wild-type and $p75^{NTR-/-}$ cocultures with the same efficiency, again indicating that $p75^{NTR}$ is the functional receptor for BDNF but not for NT3.

Our results demonstrate that neurotrophins are key mediators of PNS myelination and that different receptors are implicated in the positive and negative modulation by BDNF and NT3, respectively. A model illustrating their roles during myelination is depicted in Fig. 4. The binding of neurotrophins to $p75^{NTR}$ and Trk receptors activates divergent intracellular pathways, with Trk receptors preferentially activating prosurvival and mitogenic pathways (*2*). NT3 has been described as a prosurvival factor for SCs (*16*) and could, therefore, be acting like other ligands of tyrosine kinase receptors, such as neuregulins or fibroblast growth factor 2, by keeping the SCs in a proliferative, premyelinogenic state (*5*). On the other hand, less is known about the roles of $p75^{NTR}$. Most of the studies have focused on its pro- and anti-apoptotic functions in neurons and the intracellular signaling pathways that are activated after NGF binding (*2*, *17*). Although our results show that mature forms of neurotrophins modulate myelination, it may be possible that secreted proneurotrophins, which act as $p75^{NTR}$-specific ligands (*18*), could also regulate myelination through $p75^{NTR}$. The complete ablation of all $p75^{NTR}$ isoforms (*19*), including a splice variant that is unable to bind neurotrophins, produces a larger decrease in the number of neurons and SCs present in the sciatic nerve compared with the traditional $p75^{NTR-/-}$ mice. This suggests an additional neurotrophin-independent role for this receptor. It remains unknown whether this potential role is accompanied by a greater decrease in myelin. The DRG neurons used in this study were maintained in NGF and the sensory fibers that grew and survived were NGF dependent, which can constitute yet another layer of complexity in the interplay of neurotrophins and their receptors. Whether NGF and TrkA signaling contributes to myelination remains to be determined.

Our results offer an example of how neurotrophins promote different effects according to whether $p75^{NTR}$ or Trk is activated. Other instances in which such behavior has been documented include cell death or survival decisions in different neuronal types (*2*) and the differential regulation of neurotransmitter release by sympathetic neurons that produces a switch between excitatory and inhibitory neurotransmission (*20*).

An interesting characteristic of $p75^{NTR}$ is its high level of expression in SCs during development and in demyelination and remyelination paradigms (*21*). After nerve injury, the increase in $p75^{NTR}$ expression is accompanied by an upregulation of BDNF (*22*) and a decrease in NT3 expression (*10*). Aside from any effects on neuronal survival and axonal regrowth, these responses might also indicate a function in the myelination program. Our results indicating that $p75^{NTR}$ regulates the myelination process in the PNS allow for the possibility of using specific $p75^{NTR}$ agonists as therapeutic agents in instances in which increased myelination is required, such as peripheral neuropathies or nerve injury. Such compounds could mimic the promyelinating effects of BDNF without adverse collateral consequences in its neuronal counterparts.

References and Notes

1. M. J. Radeke, T. P. Misko, C. Hsu, L. A. Herzenberg, E. M. Shooter, *Nature* **325**, 593 (1987).
2. E. J. Huang, L. F. Reichardt, *Annu. Rev. Neurosci.* **24**, 677 (2001).
3. S. P. Squinto *et al.*, *Cell* **65**, 885 (1991).
4. D. M. Valenzuela *et al.*, *Neuron* **10**, 963 (1993).
5. G. Zanazzi *et al.*, *J. Cell Biol.* **152**, 1289 (2001).
6. B. Stevens, R. D. Fields, *Science* **287**, 2267 (2000).
7. H. L. Koenig *et al.*, *Science* **268**, 1500 (1995).
8. E. Parmantier *et al.*, *Neuron* **23**, 713 (1999).
9. J. R. Chan, J. M. Cosgaya, Y. J. Wu, E. M. Shooter, *Proc. Natl. Acad. Sci. U.S.A.* **98**, 14661 (2001).
10. H. Funakoshi *et al.*, *J. Cell Biol.* **123**, 455 (1993).
11. M. E. Sebert, E. M. Shooter, *J. Neurosci. Res.* **36**, 357 (1993).
12. Materials and methods are available as supplementary material on *Science* Online.
13. G. Weskamp, L. F. Reichardt, *Neuron* **6**, 649 (1991).
14. H. Kang, A. A. Welcher, D. Shelton, E. M. Schuman, *Neuron* **19**, 653 (1997).
15. K. F. Lee *et al.*, *Cell* **69**, 737 (1992).
16. C. Meier, E. Parmantier, A. Brennan, R. Mirsky, K. R. Jessen, *J. Neurosci.* **19**, 3847 (1999).
17. P. Roux, P. Barker, *Prog. Neurobiol.* **67**, 203 (2002).
18. R. Lee, P. Kermani, K. K. Teng, B. L. Hempstead, *Science* **294**, 1945 (2001).
19. D. von Schack *et al.*, *Nature Neurosci.* **4**, 977 (2001).
20. B. Yang, J. D. Slonimsky, S. J. Birren, *Nature Neurosci.* **5**, 539 (2002).
21. R. Heumann *et al.*, *Proc. Natl. Acad. Sci. U.S.A.* **84**, 8735 (1987).
22. M. Meyer, I. Matsuoka, C. Wetmore, L. Olson, H. Thoenen, *J. Cell Biol.* **119**, 45 (1992).

23. We thank Regeneron Pharmaceuticals, L. Reichardt, A. Welcher, and J. Archelos for reagents and antibodies; N. Ghori for expertise with electron microscopy; and B. Barres for critical reading of the manuscript. Supported by grants from NIH (NS04270), the Muscular Dystrophy Association, and the McGowan Charitable Trust (E.M.S.).

Supporting Online Material

www.sciencemag.org/cgi/content/full/298/5596/1245/DC1

Materials and Methods

References and Notes

25 July 2002; accepted 17 September 2002

Reactivation of Ocular Dominance Plasticity in the Adult Visual Cortex

Tommaso Pizzorusso,[1,2]* Paolo Medini,[1] Nicoletta Berardi,[2,4] Sabrina Chierzi,[3] James W. Fawcett,[3] Lamberto Maffei[1,2]

In young animals, monocular deprivation leads to an ocular dominance shift, whereas in adults after the critical period there is no such shift. Chondroitin sulphate proteoglycans (CSPGs) are components of the extracellular matrix (ECM) inhibitory for axonal sprouting. We tested whether the developmental maturation of the ECM is inhibitory for experience-dependent plasticity in the visual cortex. The organization of CSPGs into perineuronal nets coincided with the end of the critical period and was delayed by dark rearing. After CSPG degradation with chondroitinase-ABC in adult rats, monocular deprivation caused an ocular dominance shift toward the nondeprived eye. The mature ECM is thus inhibitory for experience-dependent plasticity, and degradation of CSPGs reactivates cortical plasticity.

Cortical circuits are sensitive to experience during well-defined intervals of early postnatal development called critical periods (*1*). After the critical period, plasticity is reduced or absent. Monocular deprivation (MD) is a classic model of experience-dependent plasticity. MD during the critical period results in a shift of ocular dominance (OD) of cortical neurons in favor of the nondeprived eye (*2*, *3*). No OD shift is seen after MD in adult

animals. The factors responsible for the cessation of OD plasticity in adults are only partially known. There is some evidence that the developmental increase in intracortical inhibition reduces plasticity and contributes to the termination of the critical period (*4–6*). However, other factors present in the adult visual cortex could stabilize synaptic connections and limit experience-dependent plasticity. CSPGs are attractive candidates for this role. CSPGs are components of the ECM that inhibit axonal sprouting and growth (*7–9*). Their adult pattern of expression is reached during late development, when CSPGs condense around the soma and dendrites of a subset of neurons in the form of perineuronal nets (PNNs) (*10*, *11*). For instance, CSPGs recognized by the CAT-301, -315, and -316 antibodies appear in the cat visual cortex around the end of the critical period and their expression is regulated by visual experience (*12*).

If CSPGs in PNNs are involved in limiting OD plasticity in adults, the formation of adult-like PNNs around visual cortical neurons should coincide with the end of the critical period. We examined PNN formation using wisteria floribunda agglutinin (WFA), which binds the CSPG glycosaminoglycan (GAG) chains, and an antibody to the NH_2-terminal fragment of the CSPG neurocan, which is associated with PNNs (*13*). During the critical period [postnatal day 22 (P22)], very few neurons were surrounded by PNNs although CSPGs were diffusely distributed (Fig. 1, A and B). The number of PNNs strongly increased in all cortical layers at P35 and reached adult levels at P70, coincident with the end of the critical period. Perineuronal staining for neurocan also increased, a process that continued during adulthood (Fig. 1, A and C). PNNs were more numerous in layer 4 than in supragranular and infragranular layers either during or after the end of the critical period (*14*). As in other brain structures, most (77 ± 1%, n = 3 rats) of the cortical neurons possessing PNNs use γ-aminobutyric acid (GABA) as a neurotransmitter, as shown by double staining with antibodies to the GABA-containing marker parvalbumin (*15*).

Rearing animals in complete darkness from birth prolongs the critical period for OD plasticity. We tested whether dark rearing (DR) up to P70 would inhibit the developmental maturation of PNNs (*12*). Condensation of neurocan into PNNs was almost completely prevented by DR (Fig. 1, E and F), although diffuse neurocan immunoreactivity was unaffected (*14*). The effect of DR appeared specific for visual cortical areas, because DR did not affect neurocan labeling in a nonvisual area (the retrosplenial cortex) located in the same sections used for the counts in the visual cortex. DR also caused a reduction in the number of PNNs in the deep and superficial layers, but not in layer 4 (Fig. 1G). Reintroducing dark-reared animals into a normal light/dark cycle rapidly terminates OD plasticity. One week of normal visual experience after DR completely restored neurocan immunoreactivity in PNNs to control values (Fig. 1, E and F).

These results, together with the known inhibitory properties of CSPGs toward axonal sprouting, prompted us to test whether the presence of CSPGs in the adult visual cortex inhibits experience-dependent plasticity. Much of the inhibitory activity of CSPGs toward axon growth can be prevented by degradation or inhibition of GAG chain syn-

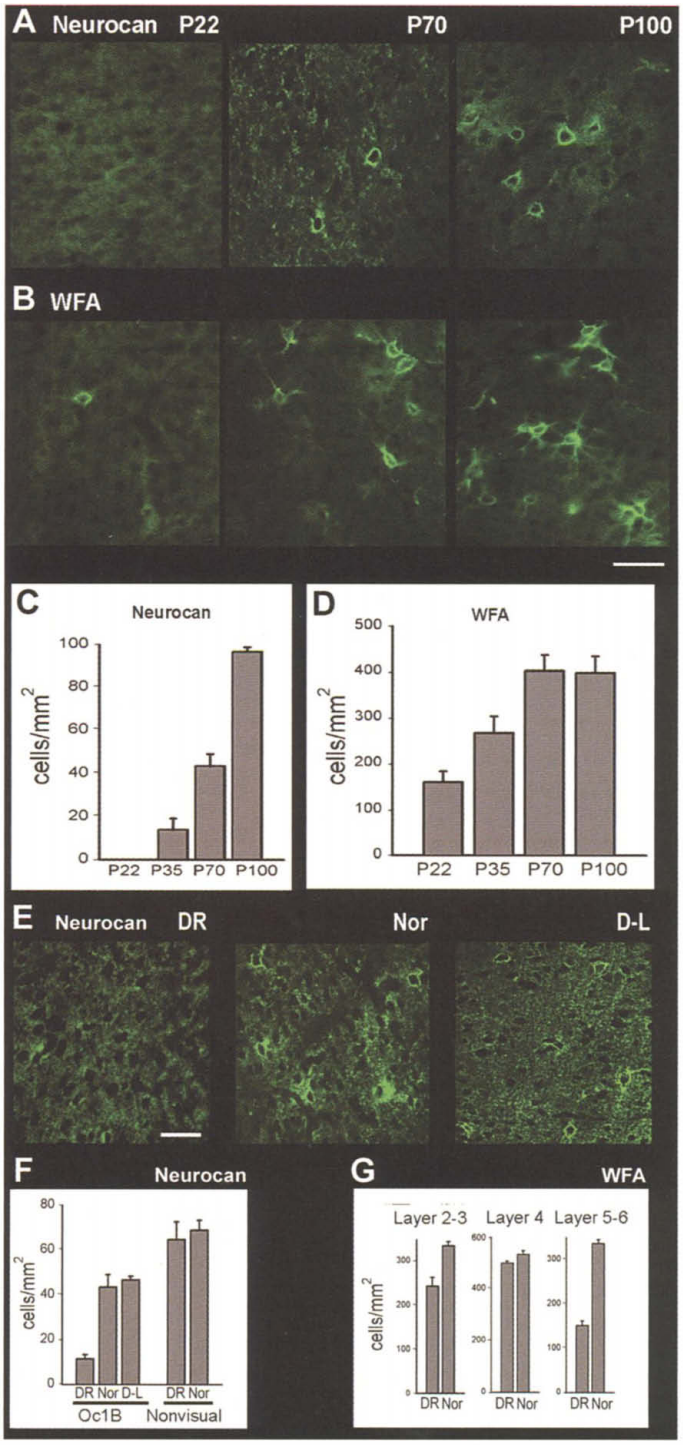

Fig. 1. Neurocan and WFA staining increases throughout the critical period and is decreased by DR. (**A**) Neurocan and (**B**) WFA staining in the primary visual cortex (Oc1b) of P22, P70, and P100 animals. (**C** and **D**) Density of cells positive for (C) Neurocan and (D) WFA in Oc1b at different developmental stages (P22 rats, n = 3; P35, n = 4; P70, n = 3; P100, n = 3). For both kinds of staining, there is a significant effect of age [one-way analysis of variance (ANOVA), $P < 0.05$] (**E**) Neurocan staining in the visual cortex of P70 dark-reared rats (DR, left), age-matched controls (Nor, center), and dark-reared rats reexposed to light for 7 days (D-L, right). (**F**) Quantitation of neurocan-positive cells in the same groups (DR, n = 4; Nor, n= 4; D-L, n = 2). The first three bars (Oc1b) refer to density values measured in Oc1b, whereas the last two (Nonvisual) refer to values measured in a nonvisual area. The density of positive cells in the Oc1b of dark-reared rats is statistically different from that in both the Nor and D-L groups (one way ANOVA, post-hoc Tukey test, $P < 0.01$). No difference is present between the Nor and DR groups in the nonvisual area (Student's t test, $P > 0.05$). (**G**) The density of WFA-positive cells in dark-reared (n = 4) and control (n = 4) rats is statistically different in layers 2 to 3 and 5 to 6 (t test, $P < 0.05$ and $P < 0.01$, respectively). Scale bar, 50 μm.

[1]Scuola Normale Superiore, 56100 Pisa, Italy. [2]Istituto di Neuroscienze, Consiglio Nazionale Ricerche, via Moruzzi 1, 56100 Pisa, Italy. [3]Cambridge University Centre for Brain Repair, Robinson Way, Cambridge CB2 2PY, UK. [4]Dipartimento di Psicologia, Università di Firenze, 50123 Firenze, Italy.

*To whom correspondence should be addressed. E-mail: tommaso@in.pi.cnr.it

thesis (*16*, *17*). Degradation of CSPG GAG chains in vivo with chondroitinase-ABC (chABC) reduces the inhibitory properties of the damaged central nervous system (CNS) sufficiently to promote axon regeneration (*18*, *19*). We intracortically injected the adult visual cortex of rats with chABC every 3 days (*14*). Seven days after the first chABC injection, immunohistochemistry using 2B6, an antibody that selectively labels digested CSPGs, showed a complete removal of GAG chains over the primary visual cortex (area Oc1b, Fig. 2A). Neurocan staining in PNNs, staining of diffusely distributed neurocan (Fig. 2A), and binding of WFA (*15*) were also not present in the chABC-treated area. Control injections of penicillinase, an enzyme with no endogenous substrate, did not affect CSPG integrity (*14*). Treatment with chABC had no effect on neuronal or astrocytic survival (*14*, *20*). We also controlled inflammatory response to the treatments using OX42, an antibody that reveals microglia and neutrophils. Penicillinase and chABC injections increased the number of hypertrophic microglia around the injection sites, but the appearance and number of OX42-positive cells within the recording zone in Oc1b [which is at least 1 mm away from the injection sites (*14*)] were not different from normal (Fig. 2, B and C).

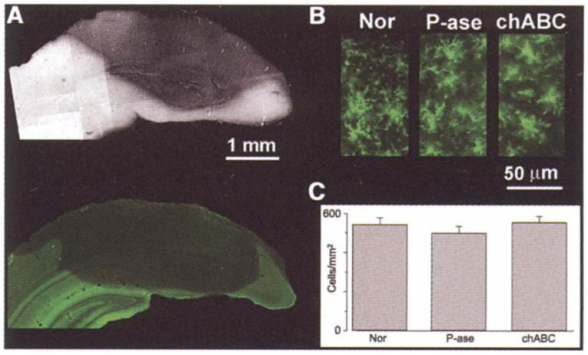

Fig. 2. Effects of chABC injection into the visual cortex. (**A**) 2B6 (top) and neurocan (bottom) staining after chABC treatment show CSPG degradation in the visual cortex treated with chABC. (**B**) OX42 staining of microglia in Oc1b of normal rats or rats injected with penicillinase (P-ase) or chABC. Inflammatory reaction to chABC or penicillinase injections was minimal within area Oc1b. (**C**) Density of OX42-positive cells in Oc1b of the three groups (n = 3 animals for each group) is not significantly different (one-way ANOVA, $P > 0.05$).

OD plasticity was assessed in adult (>P100) rats well after the end of the critical period. One eye was closed at the time of the first injection with chABC or penicillinase. The effectiveness of MD in shifting OD distribution was assessed after 7 or 15 days of MD by extracellular recordings of single-unit activity in the treated cortex (contralateral to the deprived eye). Cortical neuronal activity in untreated rats of the same age, either monocularly deprived or nondeprived, was also recorded. OD was attributed to each neuron according to the Hubel and Wiesel classification system or by computation of an OD score (*14*, *21*, *22*). Seven days of MD were totally ineffective in shifting OD distributions in adult rats who were either untreated or treated with penicillinase (Fig. 3, A through D). By contrast, a pronounced shift of OD toward the ipsilateral, nondeprived eye was induced in rats treated with chABC (Fig. 3, E to G). Fifteen days of MD did not further increase the OD shift induced by 7 days of MD in the chABC-treated rats (Fig. 3, E to G). The OD distribution of the animals in each different group was summarized with the contralateral bias index (CBI) (*6*, *23*), on which 0 represents complete ipsilateral dominance and 1 represents complete contralateral dominance. The CBIs of all rats treated with chABC were reduced with respect to normal rats or control monocularly deprived rats (Fig. 3H). To investigate whether CSPGs are involved in very early events activated by MD, we studied the effects of 2 days of MD. During the critical period (beginning at P22 to P23), 2 days of MD induced a nonsaturating shift of OD (CBI, 0.38 ± 0.03; four animals, 96 cells). MD of the same duration did not affect OD in adult rats treated with chABC (CBI, 0.6 ± 0.04; four animals, 82 cells).

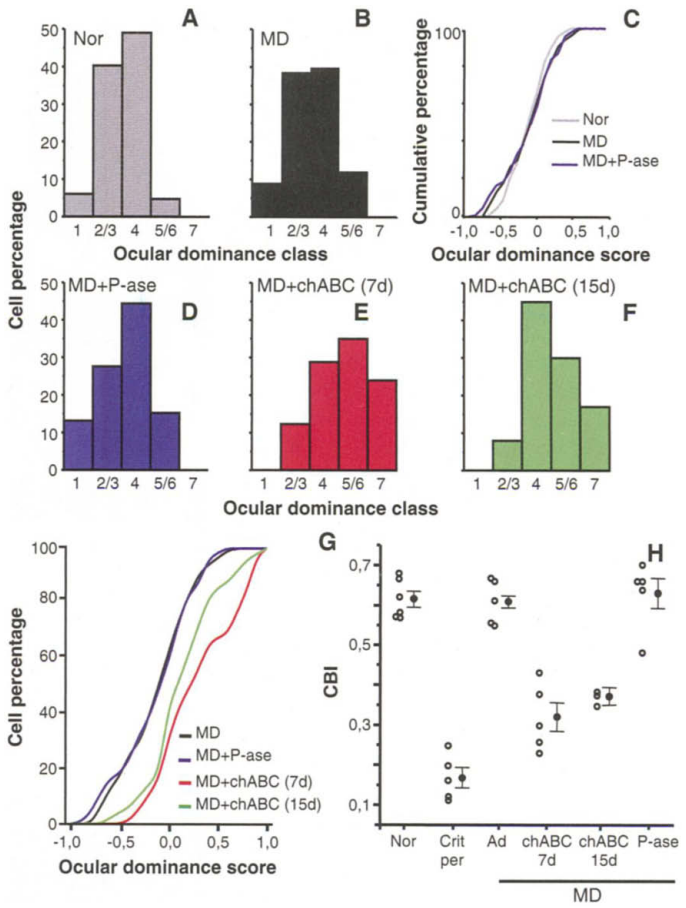

Fig. 3. CSPG degradation restores OD plasticity in the adult visual cortex. (**A** to **D**) MD has no effect in adult rats. OD distributions of (A) adult rats left nondeprived (Nor, six rats, 149 cells) or MD for 7 days either (B) untreated (MD, five rats, 163 cells) or (D) treated with penicillinase (MD + P-ase, five rats, 185 cells) are not statistically different (χ^2 test, $P > 0.05$). (C) Statistical comparison of the cumulative distributions of the OD score confirms that MD has no effect in adult rats either untreated or treated with penicillinase [Kolmogorov-Smirnov (K-S) test, $P > 0.05$; Nor, 114 cells; MD, 115 cells; MD + P-ase, 127 cells]. (**E** and **F**) chABC treatment of the visual cortex of adult MD rats for (E) 7 days (MD + chABC 7d, five rats, 120 cells) or (F) 15 days (MD + chABC 15d, three rats, 73 cells) restores an OD shift. OD distributions of animals treated with chABC for 7 or 15 days significantly differ from those of the MD + P-ase, Nor, and MD groups (χ^2 test, $P < 0.05$). (**G**) Cumulative distribution of the OD score of MD, MD + P-ase, and MD + chABC treatment groups (7 days, 74 cells; 15 days, 49 cells). MD + chABC groups are statistically different from the MD and the MD + P-ase groups ($P < 0.05$, K-S test). No difference is present between the MD + chABC groups treated for 7 or 15 days ($P > 0.05$, K-S test). (**H**) The CBIs (*23*) of normal rats, rats monocularly deprived for 7 days during the critical period (Crit per), adult monocularly deprived rats (Ad), and adult monocularly deprived rats treated with penicillinase or chABC for 7 or 15 days. Solid circles represent the average CBI ± SEM; open circles represent the CBI of single rats. The CBIs of MD + chABC 7d and 15d rats are statistically different from those of MD + P-ase, Nor, and MD rats (one-way ANOVA, $P < 0.001$; post-hoc Tukey test, $P < 0.05$), whereas these latter groups do not differ among each other.

Treatment with chABC but without MD did not cause a shift of OD toward the ipsilateral eye (Fig. 4A). Functional properties of visual cortical neurons (Fig. 4, B and C) in chABC-treated rats (either nondeprived or

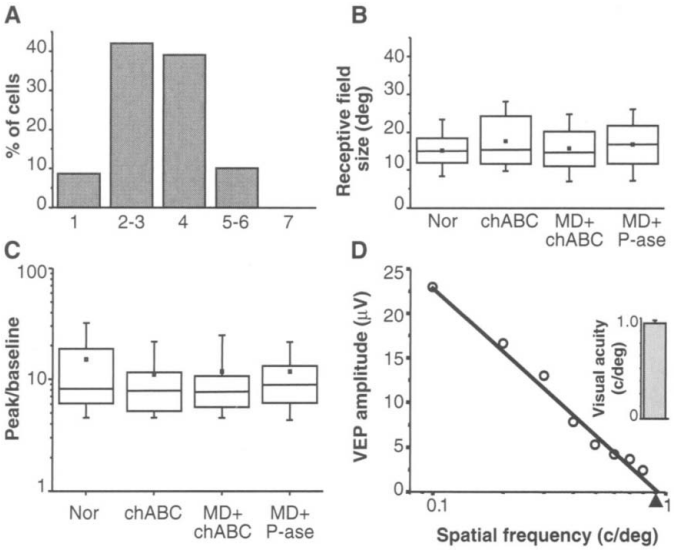

Fig. 4. chABC per se does not alter OD and other functional properties of visual cortical neurons. (**A**) OD distribution of adult rats treated with chABC for 7 days without MD (chABC, four rats, 68 cells). This distribution does not differ from that of normal rats (χ^2 test, $P > 0.05$). (**B**) Receptive field (RF) size was not altered by penicillinase or chABC in either monocularly deprived or nondeprived rats (Nor, 79 cells; chABC, 54 cells; MD + chABC, 7 and 15 days, 112 cells; MD + P-ase, 109 cells). Data are represented as box charts: Horizontal lines denote the 25th, 50th, and 75th percentiles; error bars denote the 5th and 95th percentiles; square symbol denotes mean value. None of the treatments significantly altered RF size (one-way ANOVA on ranks, $P = 0.186$). (**C**) Cell responsiveness for each unit of the different treatment groups (Nor, 93 cells; chABC, 47 cells; MD + chABC, 116 cells; MD + P-ase, 109 cells) was expressed as peak response compared with baseline activity. No statistical difference is present between all groups (one-way ANOVA on ranks, $P = 0.218$). (**D**) Normal visual acuity after 7 days of chABC treatment of adult nondeprived rats. A representative example of visual acuity measurement in a chABC-treated rat by means of visually evoked potentials (VEPs) is shown. Estimated visual acuity is indicated on the abscissa by an arrowhead. Visual acuity of chABC-treated animals (0.95 ± 0.05 cycle/deg, $n = 3$ animals, inset) is within normal values, either estimated with VEPs or behaviorally [about 1 cycle/deg (*3*)].

monocularly deprived) were not different from those of normal adult rats or control rats. Visual acuity was also not affected (Fig. 4D). This indicates that chABC treatment restored OD plasticity without interfering with many important functional properties of cortical neurons.

Our results show that degradation of CSPG GAG chains restores OD plasticity in the adult visual cortex, demonstrating that the mature ECM is a crucial factor in regulating experience-dependent plasticity. The condensation of CSPGs into PNNs correlates with the end of the critical period for OD plasticity and is prolonged by DR. This suggests that CSPG assembly in PNNs is important for the restriction of OD plasticity to the critical period.

How can CSPG removal restore OD plasticity to the adult visual cortex? CSPG inhibitory action on axonal sprouting suggests that degradation of PNNs could remove nonpermissive substrates for experience-dependent generation or rearrangement of synaptic connections, two processes that are thought to underlie cortical plasticity (*24–26*). Another possible mechanism is suggested by colocalization of PNNs with parvalbumin-positive GABA-containing interneurons. Maturation of GABA-containing interneurons has been proposed to terminate the critical period for OD plasticity. Indeed, a reduction of inhibitory transmission in the adult cortex reactivates OD plasticity (*27*). Treatment with chABC did not alter several functional properties of visual cortical neurons that are known to be affected by pharmacological treatments with GABA antagonists (*28*), indicating that general disinhibition of cortical neurons is not the mechanism by which chABC reactivates OD plasticity. Further experiments are needed to understand whether CSPGs modulate plasticity by curbing the experience-dependent formation of new synapses on and by inhibitory neurons.

Because PNNs are found throughout the CNS, targeting the PNN-forming CSPGs could be a promising strategy to promote plastic mechanisms underlying recovery from amblyopia in the visual system (*29*), as well as from many forms of damage in many parts of the CNS. Recent experiments in which rat spinal cord injuries were treated with chABC showed behavioral improvements that may have been partly due to increased plasticity (*19*).

References and Notes

1. N. Berardi, T. Pizzorusso, L. Maffei, *Curr. Opin. Neurobiol.* **10**, 138 (2000).
2. T. N. Wiesel, D. H. Hubel, *J. Neurophysiol.* **28**, 1029 (1965).
3. M. Fagiolini, T. Pizzorusso, N. Berardi, L. Domenici, L. Maffei, *Vis. Res.* **34**, 709 (1994).
4. Z. J. Huang *et al.*, *Cell* **98**, 739 (1999).
5. A. Kirkwood, H. K. Lee, M. F. Bear, *Nature* **375**, 328 (1995).
6. T. K. Hensch *et al.*, *Science* **282**, 1504 (1998).
7. J. W. Fawcett, R. A. Asher, *Brain Res. Bull.* **49**, 377 (1999).
8. M. T. Fitch, J. Silver, *Cell Tissue Res.* **290**, 379 (1997).
9. M. Grumet, D. R. Friedlander, T. Sakurai, *Perspect. Dev. Neurobiol.* **3**, 319 (1996).
10. G. Bruckner *et al.*, *J. Comp. Neurol.* **428**, 616 (2000).
11. G. Koppe, G. Bruckner, K. Brauer, W. Hartig, V. Bigl, *Cell Tissue Res.* **288**, 33 (1997).
12. C. Lander, P. Kind, M. Maleski, S. Hockfield, *J. Neurosci.* **17**, 1928 (1997).
13. F. Matsui *et al.*, *Brain Res.* **790**, 45 (1998).
14. Materials and methods are available as supporting material on *Science* Online.
15. T. Pizzorusso *et al.*, data not shown.
16. R. J. McKeon, A. Höke, J. Silver, *Exp. Neurol.* **136**, 32 (1995).
17. L. Smith-Thomas *et al.*, *J. Cell Sci.* **108**, 1307 (1995).
18. L. D. F. Moon, R. A. Asher, K. E. Rhodes, J. W. Fawcett, *Nature Neurosci.* **4**, 465 (2001).
19. E. J. Bradbury *et al.*, *Nature* **416**, 636 (2002).
20. G. Bruckner *et al.*, *Exp. Brain Res.* **121**, 300 (1998).
21. C. D. Rittenhouse, H. Z. Shouval, M. A. Paradiso, M. F. Bear, *Nature* **397**, 347 (1999).
22. OD scores were calculated as follows: {[peak(ipsi) – baseline(ipsi)] – [peak(contra) – baseline(contra)]}/{[peak(ipsi) – baseline(ipsi)] + [peak(contra) – baseline(contra)]}, where peak is the maximal spike frequency evoked by visual stimulation, ipsi is the ipsilateral eye, baseline is the mean spiking frequency in the absence of stimulation, and contra is the contralateral eye.
23. CBIs were calculated as follows: {[N(1) – N(7)] + 1/2[N(2-3) – N(5-6)] + N(tot)}/2N(tot), where N(tot) is the number of recorded cells, N(i) is the number of cells in class i, and i is the Hubel and Wiesel OD class number (1, 2 and 3, 5 and 6, or 7).
24. B. Lendvai, E. A. Stern, B. Chen, K. Svoboda, *Nature* **404**, 876 (2000).
25. E. A. Stern, M. Maravall, K. Svoboda, *Neuron* **31**, 305 (2001).
26. J. T. Trachtenberg, M. P. Stryker, *J. Neurosci.* **21**, 3476 (2001).
27. A. Harauzov, G. DiCristo, N. Berardi, L. Maffei, *Soc. Neurosci. Abstr.* **27**, 10 (2001).
28. A. S. Ramoa, M. A. Paradiso, R. D. Freeman, *Exp. Brain Res.* **73**, 285 (1988).
29. P. C. Kind *et al.*, *Nature* **416**, 430 (2002).

30. Supported by Programmi scientifici di interesse nazionale of the Ministero Istruzione Università Ricerca, Consiglio Nazionale Ricerche project SP-5, Progetto Strategico Neuroscienze, the Wellcome Trust, the Medical Research Council, and the International Spinal Research Trust. S. Landi helped with some experiments.

Supporting Online Material

www.sciencemag.org/cgi/content/full/298/5596/1248/DC1
Materials and Methods
References and Notes

9 April 2002; accepted 21 August 2002